LA-UR- 89-1162

Received by OSTI

MAY 0 9 1989



TITLE STUDIES OF THE Ag/Cu(110) BIMETALLIC INTERFACE USING OPTICAL SECOND-HARMONIC GENERATION

LA-UR--89-1162

DE89 011195

AUTHOR(S) Ross E. Muenchausen, MST-7
Mark A. Hoffbauer, CLS-2
Thomas N. Taylor, CLS-2

SUBMITTED TO Advanced Materials Institute Conference Proceedings
Denver, Colorado
March 6-9, 1989

## DISCLAIMER



MASTER



LOS ALAMOS Los Alamos National Laboratory
Los Alamos, New Mexico 87545

# STUDIES OF THE Ag/Cu(110) BIMETALLIC INTERFACE USING OPTICAL SECOND-HARMONIC GENERATION

Ross E. Muenchausen*, Mark A. Hoffbauer** and Thomas N. Taylor**
Los Alamos National Laboratory, Los Alamos, NM 87545
* Materials Science and Technology Division, MS E549
** Chemical and Laser Sciences Division, MS G738

## Introduction

Optical second harmonic generation (SHG) has recently been shown to be a sensitive, real-time, *in situ* probe for studying interfaces under many different environments[1]. With regard to atomically clean well-characterized surfaces , SHG has been shown to be sensitive to submonolayer coverages of adsorbates [2,3], the structural symmetry or molecular arrangement on the surface [4], and to surface reordering observed during laser induced melting and recrystallization [5].

Previous SHG studies of bimetallic systems have focused on alkali metal adsorption onto transition metal substrates. In these systems the observed SH response is enhanced by a factor of one thousand upon alkali adsorption, due to the large charge transfer to the substrate[6]. We have chosen to study the growth of Ag overlayers on an atomically clean and well-characterized Cu(110) surface. The Ag overlayer growth on this substrate is known to have some interesting temperature dependent behavior that is typical for systems in which significant three-dimensional clustering is known to be important [7]. Cu and Ag, while electronically similar, are immiscible near room temperature, hence there is no significant surface or bulk alloy formation [8].

## Experimental

The sample used was a ~ 10 mm dia. x 1.5 mm thick, >99.3995% pure, Cu single crystal oriented to within ~0.5° of the (110) surface. A bakeable UHV surface science apparatus (base pressure $<2\times10^{-10}$ torr) was equipped with low-energy electron diffraction (LEED) optics which could also be used in the retarding field mode to perform Auger-electron spectroscopy (AES) and work function measurements. The system was modified to allow laser beam access to the sample face and a fused-silica exit window was provided for the specularly reflected laser beams used for SHG measurements. The surface was cleaned by repeated $Ar^+$ sputtering (3 keV, ~ 10 $\mu A/cm^2$) followed by annealing in vacuum at 900K. Ag was deposited from a collimated, resistively heated vapor source operated at 1000 ±2 K and equipped with a mechanical shutter for accurately controlling the Ag dosage time. Ag was vapor deposited at base pressure of less than $3\times10^{-10}$ torr. A Ag deposition rate of approximately one Ag(111) monolayer (ML) per minute was used.

For the SHG measurements, the output of a 10 Hz pulsed Nd:YAG laser provided ~ 10 nsec pulses at 1064 nm incident on the Cu surface at an angle of ~ 68°, with the polarization vector near the [110] surface direction. Using laser fluences of ~ 100mJ/cm$^2$, which are a hundred times smaller than the reported damage threshold for Cu(110)[9b], no laser-induced surface damage heating was observed. The laser output polarization could be varied using a half wave plate to select either p- or s-input polarization relative to the surface normal. The specularly reflected SH output, ~ $10^3$photons/pulse, was separated from the fundamental using a series of glass filters with and extinction ratio greater than $10^{14}$, passed through a Glan-Taylor polarizer that could be rotated to pass only the p- or s-polarized component, and detected using a cooled PMT.

## Results

The Cu(110) surface is a corrugated low-density face consisting of rows of Cu atoms separated by troughs running in the [1$\bar{1}$0] direction. Our previous studies of Ag overlayer growth on Cu(110) using AES and LEED [9] have shown that the first Ag adatom layer is formed when Ag, initially confined along the trough direction, forms an ordered Ag(111) overlayer with the Ag-Ag nearest neighbor distance aligned across the troughs, in the [100] direction, which gives rise to the observed c(2x4) LEED pattern. Further deposition of Ag on this monolayer template was shown to have a temperature dependent overlayer growth morphology. At ~ 120K it was found that additional Ag deposition resulted in disordered layer-by-layer growth forming a continuous, though somewhat disordered, Ag film. This disordered layer growth closely approximates a Franck-van der Merwe film growth mechanism. This was in sharp contrast to the behavior observed near 300K where additional Ag deposition, between one and two monolayers, resulted in the nucleation of 3-D Ag clusters ~ 20 Å thick on top of the Ag monolayer template via a layer-cluster or Stranski-Krastanov film growth mode. With further Ag deposition, the Ag clusters were found to grow laterally across the surface and coalesce to form a continuous Ag film.

At 120K and300K the initial AES signal increases linearly indicating that a one monolayer thickness is maintained up to a Ag(111) ML coverage. Above one monolayer, the AES signals show very different behavior at the two temperatures. At 120K, the AES signal increases smoothly to a value characteristic of pure Ag at ~9 ML coverage. The 300K AES signal shows a sharp break above one monolayer coverage. The pronounced breakpoint observed above one monolayer for the 300K AES data is due to self-shadowing of the Ag from 3 D Ag crystallite formation during Ag film growth[20]. Taking the initial slope of the AES signal after the monolayer breakpoint at 300K (dashed line), and assuming an ideal clustering mode [9], we estimate that the Ag clusters nucleated on the surface are roughly 6-9 layers thick. For a Ag(111) interplanar distance of 2.35 Å this corresponds to a thickness of ~20Å. Following cluster nucleation, the addition of more Ag gives a smooth increase in the AES signal indicating lateral growth of the Ag clusters which eventually coalesce to form a continuous Ag film ~25 Å thick. At coverages above one monolayer, the LEED data are consistent with the above interpretation while also exhibiting some very complex diffraction features that will be described in detail elsewhere [10] However, it is important to note that we observe a reconstruction of the first monolayer of Ag for subsequent Ag deposition at 120K; specifically the c(2X4) pattern is replaced by a (8X1) LEED pattern between 2 3 ML.

The SH signals detected in real-time as Ag was deposited on the substrate are shown at 300 K and 120 K in figure 1. The vertical arrows indicate the Ag coverage where sharp LEED patterns were first observed. The input laser excitation was p polarized and the p polarized SH output was detected, normalized, and averaged over 30 laser pulses. The SH response has been normalized to the clean Cu(110) signal level. In all cases the SH signal initially decreases for the first ~0.5 ML of Ag deposition and then recovers to near its initial value at ~1 ML The solid lines are calculated fits to the data.

The pronounced temperature dependence of the SH response during Ag deposition is consistent with the progressive increase in the atomic scale roughness as inferred from the AES and LEED results. The enhancement of the SH signal above the clean Cu SH signal only occurs at substrate temperatures and Ag coverages where 3 D Ag nanoclusters are known to nucleate and grow[9] The general decrease in the SH output in going from clean Cu to a continous Ag film is expected since Cu is known to have interband transitions lying between 2.3 eV and a Ag film less than 200Å thick has no optical transitions below ~5 eV[11]. Therefore, the SHG from the Cu vacuum interface will be resonantly enhanced at 532 nm (2.34 eV).

Figure 2 shows the corresponding change in the work function change ($\phi$) for Ag deposition on

Cu(110) at 120K and 300K. The general decrease in $\phi$ from Cu to Ag is consistent with the reported $\phi$ values[12]. The monotonic decrease in $\phi$ beyond 1 ML Ag coverage shows no sensitivity to Ag nanoclusters. This is not surprising since these clusters have an estimated density <1% of the surface atom density[9]. The large initial slope of $\phi$ and subsequent recovery in the 0-1 ML region has been previously observed and explained in terms of island growth in several bimetallic systems. The larger initial decrease in $\phi$ at 120K is expected for film growth with a smaller average island size[13] which is consistent with a disordered layer growth mode. In contrast to previous SHG studies of adsorbate-substrate interaction[3,6] and jellium model predictions[14] which report an inverse correlation between the SH response and $\phi$, we observe a direct correlation between these quantities under our excitation conditions. As the inverse correlation between SHG and $\phi$ is only expected to hold when the free electron contribution to $\chi^{(2)}$ dominates[3], this implies that $\chi^{(2)}$ is significantly influenced by the interband electrons.

Figure 3 shows the input and output polarization dependence of SHG for subsequent room temperature depositions of Ag on Cu(110). The SHG from the s-polarized input was observed to be a factor of ~ 50 less than the SHG from the p-polarized input. However, the s-detected component of the SH output does not show the enhancement attributed to the formation of Ag nanoclusters. This is consistent with the simple idea that these 3-D, 6-atom high clusters excite surface plasmons which can only radiate in the p-polarization direction.

## Analysis

In this section we develop a simple, linear coverage dependent model for $\chi^{(2)}$, the non-linear susceptibility, which adequately describes the SH data at120 K as well as the s-detected SH data at 300 K. Subtracting away this layer growth contribution to the SH response from the p-detected, the 300K SH data gives the SH response due to the nucleation and growth of Ag nanoclusters. We can develop simple expressions for $\chi^{(2)}$ assuming layered film growth of the adsorbate as follows. For the 120K data, we write

$$\chi^{(2)}(\theta) = \chi^{(2)}_{Cu}(1 - \theta/\theta_{s1}) + \chi^{(2)}_{c(2X4)}\,\theta/\theta_{s1}, \qquad (1)$$

where $0 \le \theta \le \theta_{s1}$ and $\theta_{s1} = 1$ ML as indicated by AES and LEED results. The coverage factor in the first term of the r.h.s of eq.(1) accounts for the disappearance of the Cu interface. LEED notation has been used to label the susceptibility of the resulting bimetallic interface. For deposition of the next Ag overlayer the observed reconstruction to an (8X1) LEED pattern suggests the following expression,

$$\chi^{(2)}(\theta) = \chi^{(2)}_{c(2X4)}(\theta_{s2} - \theta)/\Delta\theta_{s21} + \chi^{(2)}_{(8x1)}(\theta - \theta_{s1})/\Delta\theta_{s21}, \qquad (2a)$$

where $\theta_{s1} \le \theta \le \theta_{s2}$, $\Delta\theta_{s21} = \theta_{s2} - \theta_{s1}$ and $\theta_{s2} = 2.5$ ML. Addition of several more Ag layers simply "buries" the existing bimetallic interface and we have for this coverage region,

$$\chi^{(2)}(\theta) = \chi^{(2)}_{(8x1)} + \chi^{(2)}_{Ag}(\theta - \theta_{s2})/\Delta\theta_{s32}, \qquad (3)$$

where $\theta_{s2} \le \theta \le \theta_{s3}$, $\Delta\theta_{s32} = \theta_{s3} - \theta_{s2}$ and $\theta_{s3} = 5$ ML. This last equation is identical to the coverage dependent $\chi^{(2)}$ proposed by previous workers to model simple substrate adsorbate interactions[1,3]. We may express the complex susceptibility for species $\Lambda$ as $\chi^{(2)}_{\Lambda} = A_\Lambda \exp(i\Lambda_\Lambda)$

so that each equationyields two fit parameters; $r_{AB} = B/A$ and $\phi_{AB} = \phi_B - \phi_A$.

For the 300K data we may again use eq.(1) for the first monolayer of Ag coverage. At coverages above 1 ML the LEED shows no significant reconstruction of the first overlayer. By analogy to eq. (2a), we have,

$$\chi^{(2)}(\theta) = \chi^{(2)}_{C(2\times4)} + \chi^{(2)}_{Ag}(\theta - \theta_{s1}) \quad \theta_{s2} \quad \theta_{s1}). \qquad (2b)$$

This represents the decay in the SH response to a continous Ag film between and 1 and 9 ML coverage. Table 1 gives the fit values for the 120K and 300K data using the layer-by-layer model. The s-detected, 300 K SH data shown in figure 3 is well described by the fit. The solid line for the p-detected, 300 K shown in figure 1 shows the resulting SH response when only this calculated layered growth contribution is considered. Unlike the previous fits, large differences are evident in the 1-8 ML region, which must correlate to the nucleation and growth of Ag nanoclusters. Clearly, the simple coverage dependence of $\chi^{(2)}$ corresponding to a layer growth does not explain the SH response for layer-cluster growth.

We develop a model for the SH response to Ag nanocluster growth and coalescence by adding an additional susceptibily, $\chi^{(2)}_{cl}$ to the r.h.s. of eqn.(2b). We postulate that this term may be written as,

$$\chi^{(2)}_{cl}(\omega) = \chi^{(2)}_{pl}(\omega)\, D(\theta,K)\, L^2(K), \qquad (4)$$

where $\chi^{(2)}_{pl}(\omega)$ is the surface plasmon contribution, D is the cluster density and L is a local field factor which depend soley on K, the cluster aspect ratio [15]. The product $D(\theta,K)\, L^2(K)$ is a roughness function that effectively mediates the surface plasmon contribution. Assuming that $L(K) = aK^2$ [15], and $D = \theta n/V_{cl}$ [16], where n is the bulk density and $V_{cl}$ is the average cluster volume. From [16] we have $V_{cl} = \pi d^3/sK^2$, where d is the average cluster thickness and s is a shape dependent factor. Substituting these definitions into eqn.(4) gives

$$\chi^{(2)}_{cl}(\omega) = \chi^{(2)}_{pl}(\omega)\, A\, \theta\, K^5 / d^3, \qquad (5)$$

where A is constant for a given cluster shape. We examine eqn.(5) in two regimes; cluster maturation,i.e. early growth between 1-1.5 ML and cluster coalescence between 2-5 ML.

During cluster maturation, we assume that the cluster density, D, is constant and that the Ag coverage is proportional to the cluster thickness, $\theta \propto d$. This implies that the shape dependent aspect ratio K (defined as the ratio of the cluster thickness to the width) is also proportional to the coverage, $K \propto \theta$. This leads to predict that

$$\chi^{(2)}_{cl}(\omega) \propto \theta^4 \qquad (6a)$$

In the region of cluster coalescence, we assume, following [16], that K is constant and $d \propto \theta^{1/2}$. This leads to the expected result that $D \propto \theta^{-1/2}$ [16]and thus

$$\chi^{(2)}_{cl}(\omega) \propto \theta^{1/2} \qquad (6b)$$

Figure 4 shows the difference between the the layer contribution (solid line) and the p detected, 300 K data in figure 1, appropriately plotted to test eqns.(6). As can be seen, this model for layer-cluster enhancement to the susceptibility reasonably explains the observed, highly nonlinear coverage dependence.

## Conclusions

Optical SHG is a sensitive technique which has been used to study Ag layer and 3-D nano-cluster growth on Cu(110). We have found that SHG can be used to distinguish between different film growth modes in this bimetallic system. The SH response to film growth at 120K is well described bu a layered growth model for the coverage dependence of $\chi^{(2)}$. The deviations from this model for the SH response at 300K provide a strong fingerprint for the nucleation and growth of Ag nanometer thick clusters, which presumably arises from a surface plasmon contribution which is mediated by the cluster-induced roughness.

## References


1. Y. R. Shen, "Surface studies by optical second harmonic generation: an overview", J. Vac Sci. Technol. B 3, 1464(1985); "Surface second harmonic generation: a new technique for surface studies", Ann. Rev. Mater. Sci. 16, 69(1986)
2. D. Heskett, K. J. Song, A. Burns, E. W. Plummer, and H. L. Dai, "Coverage dependent phase transition of pyridine on Ag(110) observed by second harmonic generation", J. Chem. Phys. 85, 7490(1986).
3. S. G. Grubbs, A. M. Santini, R. B. Hall, "Optical second harmonic generation studies of molecular adsorption on Pt(111) and Ni(111)", J. Phys. Chem 92, 1419(1988).
4. S. S. Iyer, T. F. Heinz, and M. M. T. Loy, "Summary abstract: Epitaxy of monolayer silicon films studied by optical second-harmonic generation", J. Vac. Sci. Technol. B 5, 709(1987).
5 H. W. K. Tom, G. D. Aumiller, and C. H Prito-Cruz, "Time-resolved study of laser-induced disorder of Si surfaces", Phys. Rev. Lett. 60, 1438(1988).
6. K. J. Song, D. Heskett, L. Urbach, H. L. Dai, and E. W. Plummer, "Second harmonic generation from alkali thin films on Ag(110)", Mat. Res. Soc. Symp. Proc. 83, 259(1987).
7. J. A. Venables, G. D. T Spiller, and M. Hanbucken, 'Nucleation and growth of thin films", Rep. Prog. Phys 47,399(1984).
8. S.-H. Wei, A. A. Mbaye, L. G. Ferreira, and Alex Zunger, "First principles calculations of the phase diagrams of nobel metals: Cu Au, Cu-Ag, and Ag Au", Phys. Rev. B 36, 4163(1987).
9. T. N. Taylor, M A. Hoffbauer, C. J. Maggiore, and J. G. Beery, "The growth and stability of Ag layers on Cu(110)", J. Vac. Sci. Technol. A 5, 1625(1987); T. N Taylor, M. A. Hoffbauer, L Borodovsky, J. G. Beery, and C. J Maggiore, "Ag layers on Cu(110): bonding, structure, and stability", Mat Res Soc Proc. 83, 259(1987)
10. T N. Taylor, R. L. Muenchausen, and M A. Hoffbauer,submitted to Surf. Sci.
11. H. Raether, "Solid State Excitations by Electrons", Springer Tracts in Modern Physics, 38, 85(1965).
12. H. B. Michaelson, "The work function of the elements and its periodicity", J. Appl. Phys. 48, 4729(1977).
13. F. V. Albano, J. M. Heras, P. Schrammen, M. Mann and J. Holzl, "Models of the work function upon clustering; applications to experimental data", Surf. Sci. 129, 137 (1983).

14. M. Weber and A. Liebsch, "Density-functional approach to second-harmonic generation at metal surfaces", Phys. Rev. B 35, 7411(1987); Phys. Rev. B 37, 1019(1988).
15. E. J. Van Loenen, M. Iwami, R. M. Tromp and J. F. Van der Veen, "The Adsorption of Ag on the Si(111) 7x7 Surface at Room Temperature Studied By Medium Ion Scattering, LEED and AES", Surf. Sci. 137,1 (1984).
16. A. Woukan, "Surface enhanced electromagnetic processes", Solid State Physics 38, 223(1984).

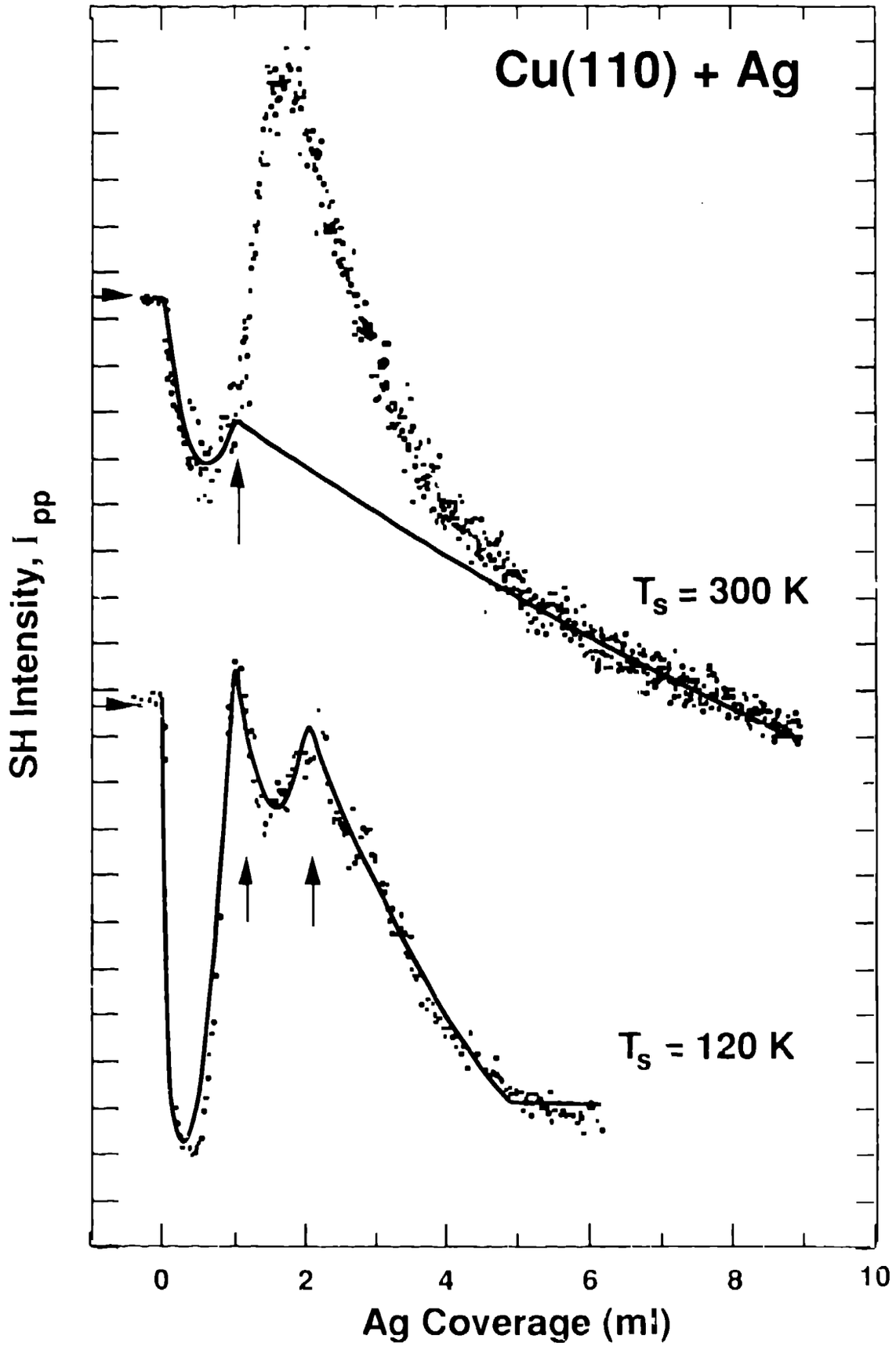


Figure 1. Surface SH signals as a function of surface coverage on Cu(110) at substrate temperatures of 120 K and 300 K. The solid lines are model fits to the data.

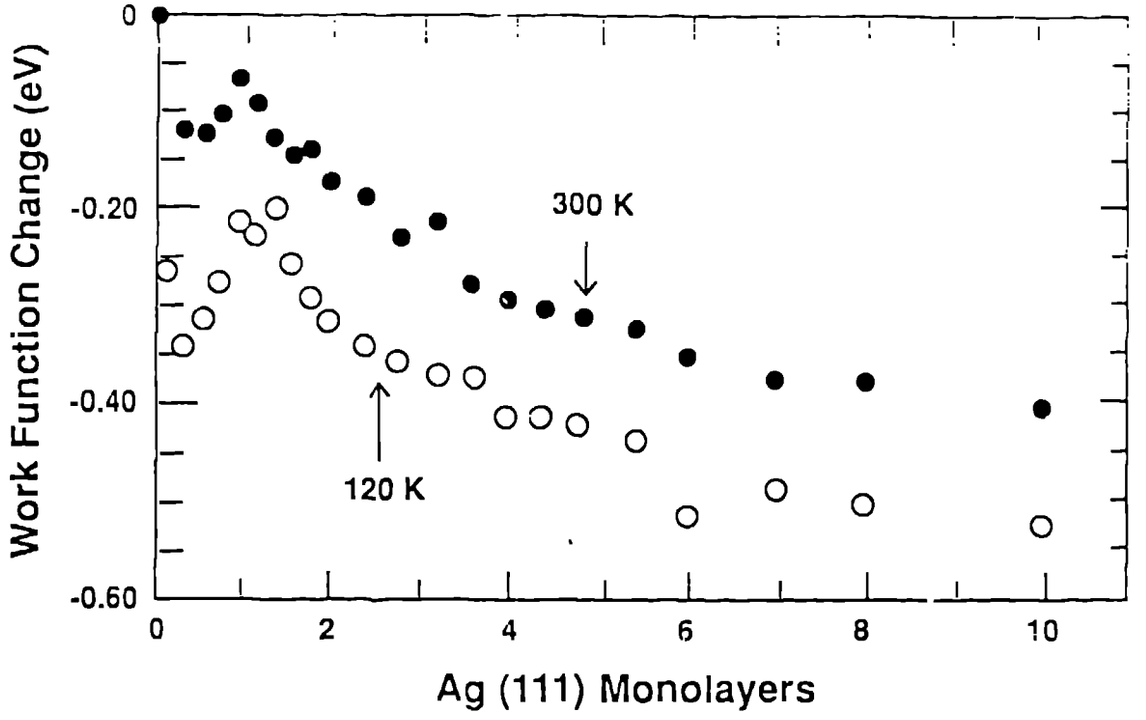


Figure 2. Work function change as a function of surface coverage on Cu(110) at substrate temperatures of 120 K and 300 K. The s-detected SH response directly correlates with the measured work function change.

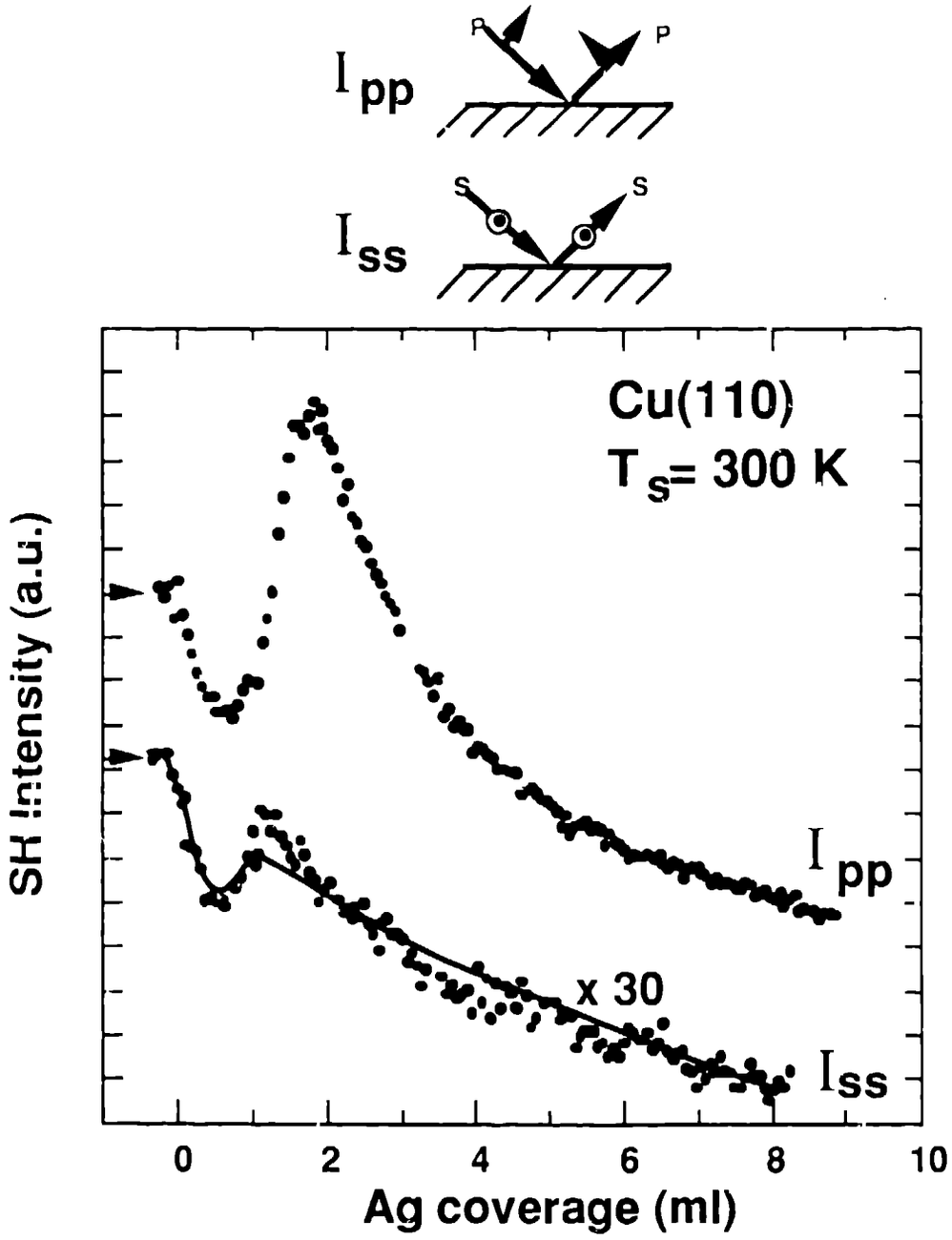


Figure 3. Surface SH signals as a function of Ag coverage on Cu(110) at 300 K for different laser polarization combinations. The 1064 nm input and 532 nm detected polarization combinations are drawn schematically at the top. The solid line is a fit to the $I_{ss}$ data.

TABLE 1.Layer-by-Layer Fit Parameters to the SHG Response From the Ag/Cu(110) System

| Fit Parameter | 120 K-SHG[a] | 300 K-SHG[b] |
|---|---|---|
| $\theta_{s1}$ | 1.0[c] | 1.0 |
| $\theta_{s2}$ | 2.5 | 9.0 |
| $\theta_{s3}$ | 5.0 | n.a.[d] |
| r1 | 0.98 | 0.9 |
| r2 | 1.0 | 0.47 |
| r3 | 0.5 | n.a. |
| $\delta 1$ | 68° | 50° |
| $\delta 2$ | 50° | 180° |
| $\delta 3$ | 160° | n.a. |

a) p-detected SH
b) s-detected SH
c) All saturation coverages are referenced to a Ag(111) monolayer.
d) Only two coverage regions were needed to fit the 300 K data.

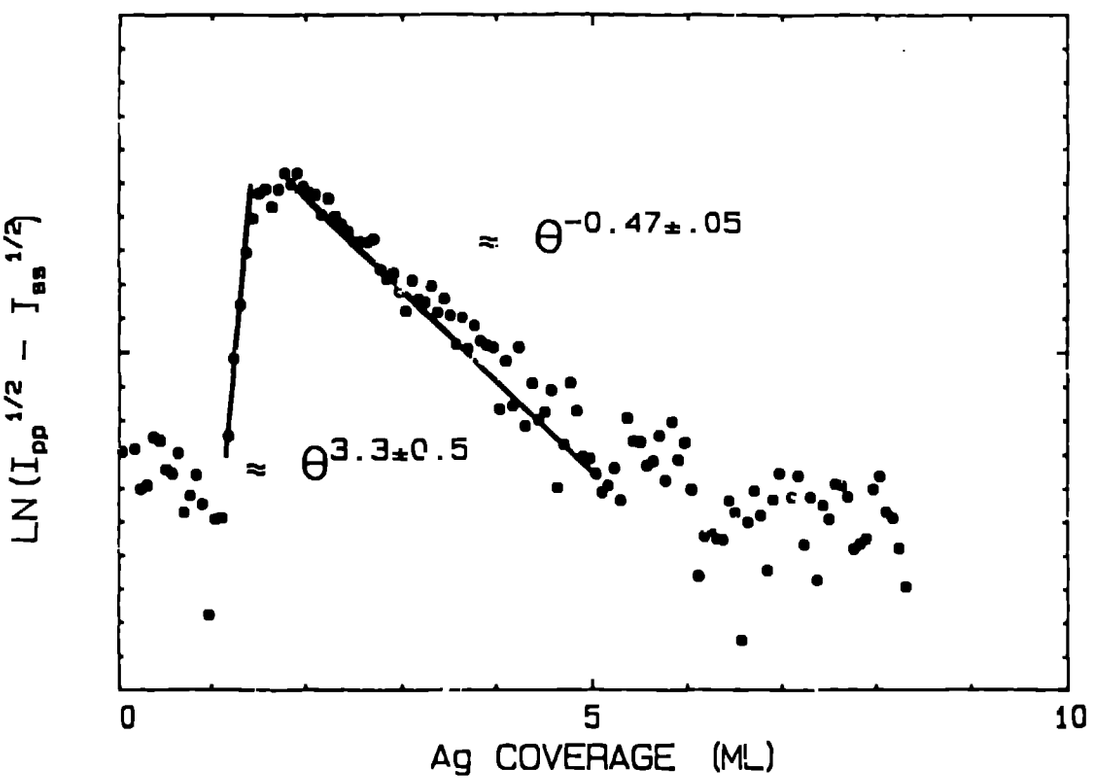


Figure 4. Coverage dependence to the susceptibility attributed to layer cluster growth for Ag on Cu(110) between 1-5 ML at 300 K. Linear fits over coverage regions associated with the maturation and coalescence of Ag clusters are in good agreement with the layer-cluster model predictions in eqn.(6).